HHS Public Access

Author manuscript

Langmuir. Author manuscript; available in PMC 2017 August 20.

Published in final edited form as:

Langmuir. 2015 February 17; 31(6): 2036–2042. doi:10.1021/la5044156.

Effects of Temperature on the Morphological, Polymeric, and Mechanical Properties of *Staphylococcus epidermidis* Bacterial Biofilms

Leonid Pavlovsky[†], **Rachael A. Sturtevant**[‡], **John G. Younger**[‡], and **Michael J. Solomon**[†]

[†]Department of Chemical Engineering, University of Michigan, Ann Arbor, Michigan 48109, United States

[‡]Department of Emergency Medicine, University of Michigan, Ann Arbor, Michigan 48109, United States

Abstract

Changes in temperature were found to affect the morphology, cell viability, and mechanical properties of *Staphylococcus epidermidis* bacterial biofilms. S. *epidermidis* biofilms are commonly associated with hospital-acquired medical device infections. We observed the effect of heat treatment on three physical properties of the biofilms: the bacterial cell morphology and viability, the polymeric properties of the extracellular polymeric substance (EPS), and the rheological properties of the bulk biofilm. After application of a 1 h heat treatment at 45 °C, cell reproduction had ceased, and at 60 °C, cell viability was significantly reduced. Size exclusion chromatography was used to fractionate the extracellular polymeric substance (EPS) based on size. Chemical analysis of each fraction showed that the relative concentrations of the polysaccharide, protein, and DNA components of the EPS were unchanged by the heat treatment at 45 and 60 °C. The results suggest that the EPS molecular constituents are not significantly degraded by the temperature treatment. However, some aggregation on the scale of 100 nm was found by dynamic light scattering at 60 °C. Finally, relative to control biofilms maintained at 37 °C, we observed an order of magnitude reduction in the biofilm yield stress after 60 °C temperature treatment. No such difference was found for treatment at 45 °C. From these results, we conclude that the yield stress of bacterial biofilms is temperature-sensitive and that this sensitivity is correlated with cell viability. The observed significant decrease in yield stress with temperature suggests a means to weaken the mechanical integrity of *S. epidermidis* biofilms with applications in areas such as the treatment of biofilm-infected medical devices.

Graphical abstract

Notes

The authors declare no competing financial interest.

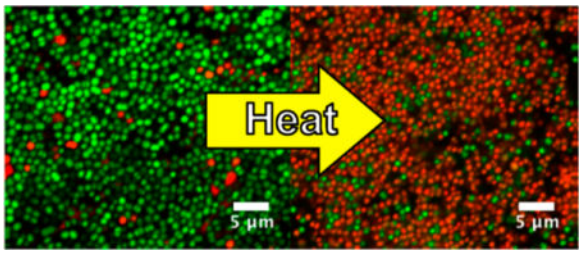

INTRODUCTION

Bacterial biofilms are multicellular communities enclosed within the matrix of an extracellular polymeric substance (EPS) that can colonize a variety of water-rich environments.[1,2] These environments range from natural hot springs and riverbeds to man-made industrial pipelines and medical devices. In these and other environments, flowing fluids impose shear stresses on the biofilms.[1–4] The EPS, composed of polysaccharides, proteins, and DNA that has been lost from cells into the local environment, is synthesized primarily by the bacterial cells.[5,6] The EPS has multiple attributes and functions, one of which is to enable the biofilm to withstand applied shear forces.[7] Another is to slow the diffusion of antimicrobial agents, allowing the bacteria to build resistance genetically.[8–11]

One such biofilm-forming bacterium of medical significance is *Staphylococcus epidermidis*. *S. epidermidis* is a normal member of the human skin flora. However, this organism is prevalent in medical device infections and is among the most common hospital-acquired bloodstream infections in the United States. The species is present in approximately 70% of all intravascular catheter-related infections.[12,13] Current antibiotic treatments to eradicate biofilms are not fully effective because antibiotics are not able to penetrate the EPS to sessile and slowly metabolizing bacteria deep within it.[8,10,14–18] Hence, infections often prompt the surgical removal and subsequent replacement of affected devices.[8,19,20] Immune-compromised patients exhibit especially high mortality rates (greater than 30%) from *S. epidermidis* infections.[5]

As strategies based on antibiotics typically fail in the treatment of infected implanted devices, we believe that the physical and mechanical properties of biofilms, not just the biochemical and genetic features, should be considered to be therapeutic targets. Previous work has determined the mechanical properties of biofilms through various methods.[21,22] The elastic modulus (G') of *S. epidermidis* biofilms, found through mechanical rheometry, varies widely, from 1 Pa to 8 kPa, depending on factors such as growth conditions and analytical methods.[23–30] Under conditions that most resemble those in which *S. epidermidis* biofilms cause disease, Pavlovsky et al.[31] determined that G' is approximately 10 Pa. In the same study a yield stress of approximately 20 Pa was reported for these biofilms. Size exclusion chromatography characterization of the polysaccharide constituent of the *S. epidermidis* EPS, called polysaccharide intercellular adhesion, found a weight-average molar mass of $(2.01 \times 10^5) \pm 1200$ g/mol. The radius of gyration of the polysaccharide was 29.2 ± 1.2 nm.[32]

The structure and mechanical properties of *S. epidermidis* biofilms depend on environmental conditions. Stewart et al.[33] showed, via confocal laser scanning microscopy (CLSM), that *S. epidermidis* biofilms adopt different density phenotypes depending on the concentration of NaCl in the growth media. The NaCl concentration and temperature impact the elastic modulus of these biofilms in an analogous way.[31] Moreover, a temperature cycle from 5 to 60 °C was found to decrease the elastic modulus of these biofilms by a factor of 3.[31]

This reported effect of temperature on the mechanical properties of biofilms is of particular interest because of its therapeutic potential. Specifically, in seeking to avoid the surgical replacement of implantable devices, altering the elasticity and yield stress of a biofilm might allow for mechanical debridement of the infection site without requiring device replacement. Because temperature can be varied within the body noninvasively, this variable's effect on biofilms' physical properties should be more comprehensively investigated. Such temperature modulation, for example, has proven effective as an adjuvant therapy for cancer.[34,35] Thus, in this article, we investigate the effect of temperature treatment on cell viability and morphology as well as the polymeric and mechanical properties of *S. epidermidis* biofilms. We hypothesize that, by exposing the biofilm to a temperature treatment, we can alter the biofilm morphology, the polymeric properties of its EPS, and the mechanical properties of the biofilm.

To study the morphology and viability of bacterial cells, we use two forms of microscopy: scanning electron microscopy (SEM) and confocal laser scanning microscopy. With scanning electron microscopy, we observe the size and surface characteristics of individual bacterial cells. Via confocal microscopy, we distinguish viable and dead cells by differential staining with fluorescent dyes.[36] We determine the weight-average molecular weight and the hydrodynamic radius of components in the EPS using size exclusion chromatography and dynamic light scattering, respectively. Finally, we use parallel plate rheometry to study the temperature dependence of the rheological properties of the biofilm in situ. The rheological properties studied are the yield stress and the elastic modulus.

METHODS AND MATERIALS

Rheometry

Biofilm Growth and Heat Treatment—A biofilm-forming clinical isolate of *S. epidermidis*, strain RP62A, was obtained from the American Type Culture Collection (culture 35984). The bacteria were incubated at 37 °C on tryptic soy agar (TSA) overnight. An individual colony was used to inoculate approximately 30 mL of a tryptic soy broth (TSB) medium supplemented with 1% D-(+)-glucose. This culture was grown overnight on a shaker table (Innova 2000 platform shaker, New Brunswick Scientific) at 200 rpm and 37 °C. The next day, 2 mL of the culture was used to inoculate glucose-supplemented TSB on a mechanical-stress-controlled rheometer (AR-G2, TA Instruments), with the Peltier plate maintained at 37 °C, as per the procedure described by Pavlovsky et al.[31] Briefly, under these conditions, the shear stress for growth was 0.1 Pa and the medium's flow rate was approximately 0.5 mL/min. The entirety of the growth phase and the evaluation of biofilm uniformity and attachment were conducted as described by Pavlovsky et al.[31]

After the growth phase, the temperature in the Peltier plate was changed to a higher temperature to stress the biofilm thermally. The temperatures used were 37, 45, and 60 °C, which correspond to the control, the maximum temperature safely applicable in the human body, and the high-temperature case in which an irreversible decrease in the biofilm elastic modulus was previously observed, respectively.[31,37] The biofilm was exposed to these temperatures for an hour, during which time the rheometer fixture was held stationary.[34,35]

Rheological Characterization of the Yield Stress—Following treatment, an oscillatory strain sweep was conducted to determine the elastic modulus (G') and yield stress of the biofilm. The strain sweep was performed at a constant oscillatory frequency of 1 Hz (6.283 rad/s) over the range of 0.01–100 dimensionless strain units. This oscillatory frequency was selected because it approximates the fundamental frequency of the human circulatory system.[38] The elastic component of the stress, τ_{Elastic}, equal to $G' \times$ strain, was plotted. The point at which τ_{Elastic} is a maximum is a well-known measure of the yield stress and strain.[39]

Cell Morphology and Viability. Confocal Laser Scanning Microscopy

Following the oscillatory strain sweep on the rheometer, biofilm samples were removed from the Peltier plate and deposited on a glass slide. The biofilm was then stained using a fluorescent staining kit (LIVE/DEAD *Bac*Light bacterial viability kit, Molecular Probes) with the dye ratio of SYTO 9 to propidium iodide to filter-sterilized deionized water of 3 μL: 3 μL:1 mL.[27,36,40] This mixture has a SYTO 9 to propidium iodide ratio of 1:6 by concentration, with approximately 3 μL of each dye premixed as required per mL of bacteria to be stained. After being stained, the sample was incubated at room temperature in the dark for 20 min and then gently rinsed with filter-sterilized deionized water and covered with a cover glass.

The sample was imaged (A1RSi confocal laser scanning microscope, Nikon) using two-channel imaging with laser wavelengths of 488 and 561 nm, consistent with the excitation spectra of the live and dead bacterial cell dyes, respectively. These channels used FITC and Texas red filters to capture the emission spectra for the live and dead cell dyes of 525 and 595 nm, respectively. The image size was 31.7 × 31.7 × 10.0 μm^3, where the voxel size was 0.062 × 0.062 × 0.062 μm^3. Image analysis was performed using custom codes that make use of the Crocker and Grier algorithm to determine the ratios of live to dead cells in a given sample.[40,41]

Scanning Electron Microscopy—In similar experiments, biofilm samples were removed from the Peltier plate, deposited on a glass coverslip, and submerged in 4% glutaraldehyde (Electron Microscope Systems).[14,42] After a minimum of 1 h, the sample was then washed and serially dehydrated in increasing concentrations of ethanol. The sample was then mounted on an SEM stub, sputter coated with gold, and imaged (AMRAY 1910 field emission scanning electron microscope, Amray Inc).

Quantitative Growth Culture—Mid-log-growth planktonic *S. epidermidis* was washed and resuspended to a final $OD_{600\ nm}$ of 0.1. Ten microliters of culture (approximately 10^5

CFU) was added to 1 mL of TSB. Samples were incubated in a dry bath incubator (Isotemp 125D, Fisher Scientific) at the desired temperature (37, 45, or 60 °C) for 1 h and then quantitatively cultured by serial dilution.

Polymer Properties

EPS Purification—After *S. epidermidis* was incubated on TSA overnight, an individual colony was isolated and used to inoculate 50 mL of TSB + 1% glucose medium in a 50 mL conical tube. This culture was grown for approximately 15 h on a shaker table at 60 rpm and 37 °C. The sample was then scraped from the tube, taking care to extract all of the biofilm, and placed in 1 L of TSB + 1% glucose medium for 24 h of growth at 60 rpm and 37 °C. After this step, a series of washing and centrifugal concentrating steps (3900g, 3 × 25 min, 4 °C) were followed as described by Ganesan et al.[32] The remaining pellet was then resuspended in 20 mL of deionized water, on which sonication was performed (8 × 30 s cycles, 60% amplitude) using a point sonicator (model 120 sonic dismembrator, Fisher Scientific) to release the polymers from the bacterial cells.[32] Centrifugation (9000g, 30 min, 12 °C) was performed to separate the polymers (supernatant) from the cells (pellet), after which the supernatant was further clarified (12 000g, 10 min). The clarified polymer was then filter sterilized and concentrated using centrifugal filters with a 10 kDa cutoff membrane (Amicon Ultra-15, Millipore). Although this filtration step may remove some low-molar-mass components of the matrix, it does collect the high-molar-mass fractions, which are the predominant contributor of the polysaccharide to the (weight-average) molar mass distribution and biofilm rheology.[32] Temperature treatment was applied using a dry bath for 1 h.

Size Exclusion Chromatography—Size exclusion chromatography (SEC) was conducted using multiple columns in series (Waters Utlrahydrogel 2000 and 250, Waters Corp.). Approximately 100 μL of sample was injected (Rheodyne) into an aqueous mobile phase of 0.1 M $NaNO_3$ and 0.05% (w/w) NaN_3, flowing at a rate of 0.45 mL/min. The outlet of the column was connected to a multiangle laser light scattering unit (MALLS; DAWN EOS, Wyatt Technology) and a concentration detector (RI; Optilab DSP interferometric refractometer, Wyatt Technology). The chemical complexity of the sample did not allow for the angle-dependent scattering intensity to be resolved as a distribution of molecular weight (Mw) and the *z*-average radius of gyration (R_g).[43,44] However, the SEC experiments do yield the mass concentration of the polymers present in each fraction eluting from the column. Chemical analysis of each fraction yielded information about any change in the relative concentration of its constituents.

Chemical Analysis—In order to determine if the mass concentration of polysaccharide, protein, or extracellular DNA components of each fraction eluting from the SEC was changing due to the heat treatment, samples that had been fractionated by SEC were collected and three chemical assays were conducted. The Smith-Gilkerson assay was used to determine the presence of *N*-acetyl-glucosamine, a major component of the polysaccharide intercellular adhesion of the biofilm.[32,45] Similarly, a bicinchoninic acid assay (BCA) was used to determine the concentration of protein, and a microvolume spectrophotometric assay

(Thermo Scientific NanoDrop 2000 spectrophotometer) was used to determine the concentrations of nucleic acid as well as protein.[46–48]

Dynamic Light Scattering—Dynamic light scattering (DLS) was performed on the specimens following heat treatment to measure the distribution of hydrodynamic radii (R_h) of species present (ALV CGS-3 compact goniometer system). The samples were diluted, if necessary, to a total volume of approximately 0.8 mL. A helium-neon laser source (JDS Uniphase Corporation) with a wavelength of $\lambda = 633$ nm was used, with the DLS detectors at a fixed angle of $\theta = 90°$. Experiments were conducted in triplicate, recording the time-dependent intensity of the scattered light for 4 min intervals after the treated biofilms had returned to room temperature. The fluctuations of the scattering intensity due to particle motion are processed with an ALV multiple-τ digital correlator (ALV-7004), giving an intensity autocorrelation function. The correlation of scattered light is then fit using a nonlinear fitting method (constrained regularization) to obtain the DLS relaxation rate which is proportional to the scattering vector $q = 4\pi n_0/\lambda \sin(\theta/2)$, where n_0 is the solvent refractive index, via the particle diffusivity, D.[49,50] Using the Stokes–Einstein relation ($D = k_B T/6\pi\eta R_h$, where k_B is Boltzmann's constant, T is temperature, and η is the viscosity), the probability distribution of effective hydrodynamic radii of the scattering specimen is then obtained.[51] Here, the refractive index and viscosity are that of water at the temperature of the measurement. The output of the measurement is the distribution function of the hydrodynamic radius of the specimen.

RESULTS AND DISCUSSION

Morphology and Viability of Bacterial Cells

Figure 1a–c reports the scanning electron micrographs of the bacterial cells following temperature treatment for 1 h at 37, 45, and 60 °C, respectively. At 37 °C, cells were of a normal size and had a smooth surface, and many were in the process of cell division, as evident by the large number of dividing planes visible.[52] At 45 °C, cell wall defects were noted and cell divisions were rare. Following treatment at 60 °C, cell surfaces were visibly roughened, which we believe is due to surface coating from the remnants of lysed cells, and there was no structural evidence of cell division. Although sample preparation for SEM imaging is known to perturb the biofilm structure because of dehydration, the glutaraldehyde fixation step may help to preserve the general shape of bacterial cells. Moreover, because the specimens subjected to different temperature treatments received the same sample preparation, comparative observations are possible.

To corroborate the SEM observations of temperature effects on cell morphology, Figure 1d–f shows CLSM imaging of the biofilms under the same three conditions. In this case, live–dead staining directly yields information about cell viability. Imaging was accomplished using two different fluorescent nucleic acid stains: SYTO 9, which penetrates both intact (i.e., live, green) and damaged (i.e., dead, red) cell membranes, and propidium iodide, which can penetrate only damaged cell membranes and displaces any SYTO 9 present. By comparing Figure 1d and Figure 1e, we cannot distinguish a difference in the proportions of

live to dead cells at these two lower treatment temperatures. However, at 60 °C, a majority of the cells (>70%) are dead. The complete SEM and CLSM results are summarized in Table 1.

Figure 1g confirms this trend. Here, a quantitative growth culture was obtained via serial dilutions of treated biofilms, and the colony-forming units (CFU) were counted. The 37 and 45 °C treatments had almost identical numbers of CFUs: 4.31 ± 1.58 ($\times 10^5$) and 4.28 ± 1.63 ($\times 10^5$), respectively. However, there was greater than a 100-fold decrease in the number of colonies present after a 60 °C treatment: 1.43 ± 0.43 ($\times 10^3$) CFU.

Polymeric Properties of EPS

In Figure 2, we report the results of refractive index (RI) detection in the size exclusion chromatography (SEC) of EPS produced by *S. epidermidis* biofilms. The RI detector signal is proportional to the mass of solute eluting from the SEC. Following EPS purification (cf. Methods and Materials), SEC was conducted on the heat-treated EPS samples. In SEC, the elution time is inversely proportional to the size and molecular weight of the sample; smaller species have longer elution times. The signal in this case is proportional to the solute concentration passing through the SEC. The concentration profile of material eluting from the SEC does not vary for the different temperature treatments. Hence, the mass fraction of differently sized species in the EPS is nearly independent of temperature. Any changes in mass fraction are smaller than can be detected by the RI instruments of the SEC system.

Four peaks in the RI signal with elution volume are apparent in Figure 2. These peaks reflect the chemical heterogeneity of the EPS. Chemical analysis of these elution fractions, as discussed subsequently, suggest that from the left to right the first two peaks are from *N*-acetyl-glucosamine while the third and fourth peaks are due to both nucleic acid and proteins. This result is consistent with Ganesan et al.[32] Moreover, the measured molar mass is consistent with the literature. Specifically, Ganesan et al.[32] found that the second peak in the refractive index distribution displayed a mean molecular mass of (2.01×10^5) ± 1200 g/mol. For comparison, the equivalent measurement for our experiments (second peak after 37 °C treatment) produces a mean molecular mass of (2.59×10^5) ± 8000 g/mol.

Figure 3a–c shows the SEC elution times of the three major chemical species of the biofilm. Fractions from the SEC were collected and assayed for the presence of *N*-acetyl-glucosamine (a), nucleic acid (b), and proteins (c) as a function of elution time from the SEC and the particular temperature treatment. The protein results are the average of two different methods, so as to address the known deficiency of such assays.[53] From these chemical assays, we learn that the mass distribution of polysaccharide, protein, and DNA in each SEC elution fraction does not change appreciably because of the temperature treatment. This finding corroborates the results of the SEC RI detector. We therefore conclude that there is no change at 60 °C in the elution time of these species, as resolved by these mass detection assays. The absence of changes in elution time suggests that none of the three molecular species analyzed for polysaccharide, protein, and DNA are undergoing significant degradation due to the temperature treatment. If degradation of one of these species had occurred, we would have expected that its mass fraction would have shifted to later times because the degraded species, now of lower molar mass, would have eluted from the SEC column more rapidly.

Figure 4 shows the probability distribution function (PDF) of the hydrodynamic radius of species detected in the purified EPS samples, as quantified by DLS. Without heat treatment (i.e., the 37 °C case), a broad distribution of hydrodynamic radii is detected in the EPS, spanning from smaller than 10 nm to greater than 100 nm. A similar trend exists for the 45 °C case, with the additional effects of a slight narrowing of the distribution and a shift toward larger hydrodynamic radii. For the 60 °C case, the distribution of hydrodynamic radii has narrowed considerably, with a pronounced peak at ~100 nm.

The 100 nm length scale that is the dominant peak detected by DLS at 60 °C is both larger than the expected size of the molecular species (e.g., PIA ~30 nm in size[32]) and smaller than the size of individual cells (e.g., *S. epidermidis* radius is ~500 nm[32,54]). A number of potential explanations for the prominent characteristic size of 100 nm in the 60 °C sample are available; however, we do not have sufficient information available to select among them. The potential explanations are (i) aggregation and (ii) cellular debris. Aggregation of the smaller components of the biofilm may be occurring as materials with $R_h < 30$ nm disappear following the 60 °C treatment. Also, the absence of particles with $R_h > 300$ nm, which are prevalent in the lower-temperature cases, may indicate cell lysis, as shown via SEM in Figure 1. In this case, the cellular debris would be smaller than the radius of the cell and may account for the increased presence of particles with $R_h \approx 100$ nm.

Yield Stress of *S. epidermidis* Biofilms

Figure 5 reports the measurement used to determine the yield stress of the *S. epidermidis* biofilms as a function of treatment temperature. An oscillatory strain sweep was conducted to measure the strain-dependent nonlinear elastic modulus. Figure 5a shows the elastic component of the stress ($\tau_{Elastic} = G' \times$ strain) plotted as a function of applied strain amplitude for the three different temperature conditions. Previous work has found that the stress maximum is a measure of the yield stress.[39] By this method, the yield stress was found to be 23.3 ± 4.4 Pa for our control case of 37 °C. This value agrees with the yield stress found in an earlier study by a different method—nonlinear biofilm creep compliance testing. The value found in that study was 18.3 ± 6.0 Pa, a difference of 27%, thereby validating the method used in the present study.[31] The long duration required for creep compliance testing (>5 h) was not conductive to studying the effects of a short-time temperature treatment. Hence, the oscillatory strain sweep method was used to reduce testing to ~5 min.

The biofilm treated at 45 °C exhibited a yield stress of 19.2 ± 6.2 Pa. This yield stress is not statistically different from the control case of $T = 37$ °C ($p = 0.60$). However, the yield stress of the biofilm treated at 60 °C was significantly lower than the control case: 3.9 ± 1.0 Pa ($p = 0.006$). This same trend is apparent in the measurements of the small strain (linear) G'. The linear elastic modulus and yield stress results are summarized in Figures 3 and 5b,c, respectively. Thus, following a 60 °C temperature treatment, the *S. epidermidis* biofilm yield occurs at a stress that is an order of magnitude smaller than in the untreated, control case. The integrity of the biofilm is therefore significantly weakened by temperature treatment.

Finally, we consider how the individual biofilm components, as quantified in Figures 1–4, might be correlated with the observed changes in mechanical properties. First, the

morphology measurements indicate that cell reproduction stops by 45 °C and cell death has occurred by 60 °C. Second, there is little change in the mass distribution of EPS constituents as a consequence of the different temperature treatments, with the exception of the appearance of a component of size 100 nm after temperature treatment at 60 °C.

Thus, cellular death and the production of an EPS species of size 100 nm are correlated with the observed decrease in biofilm yield stress at 60 °C. Furthermore, we conclude that the halt of cell replication at 45 °C is not associated with a change in yield stress because the 45 °C-treated yield stress was not significantly different than the control case. Finally, the yield stress of a mature biofilm can change without being accompanied by significant degradation of the polysaccharide, protein, and DNA components of the EPS.

CONCLUSIONS

The effects of antibiotics and antimicrobial agents on bacterial biofilm infections have received significant attention in the literature.[4,8,17,55] However, little attention has been paid to the potential role of physical methods for biofilm treatment. The physical methods that have received attention are magnetic fields, ultrasound, and pulsed electrical fields.[56–59] However, heat has been used successfully to treat certain types of cancer. Therefore, it could potentially play a role in fighting medical device infections by bacterial biofilms. To establish the scope of such a role, we have investigated the impact of heat treatment on the two main microscopic structural components of the biofilm matrix: the bacterial cells and the extracellular polymeric substance. In our experiments, we found that the application of heat caused morphological changes in the bacterial cells present in the biofilm, including a drastic decrease in cell viability when the biofilms were exposed to a treatment of 1 h at 60 °C. Additionally, a new component of size ~100 nm was formed in the EPS after heat treatment at 60 °C. Species of this size were largely absent from the control biofilms and from the biofilms treated at 45 °C. This ~100 nm species was the only change in the EPS: the chemical analysis of fractionated samples designed to monitor the chemical degradation of polysaccharide, protein, and DNA constituents of the EPS was unchanged by the temperature treatments at 45 and 60 °C.

Bulk rheological characterization correlated strongly with the ratio of live to dead cells in the bacterial biofilm. A 60 °C temperature treatment resulted in a significant decrease in the yield stress and the small strain elastic modulus of the biofilm. Thus, the effect of temperature on cell viability is implicated in the observed weakening of bacterial biofilms upon temperature treatment.

We have therefore shown that by exposing the biofilm to a local temperature treatment we can weaken the integrity of the biofilm. This reduction of the yield stress supports the idea that biofilms are mechanically weakened by short bursts at high temperature and suggests that a temperature-treated biofilm might be more easily sheared off of an infected device. If validated by future work, this finding would open the door to the treatment of biofilm infections via external means such as heat-enhanced ultrasonic vibration and would thereby ameliorate the need for surgical intervention in the treatment of biofilm infections on medical devices.

Acknowledgments

We thank Mahesh Ganesan for his assistance with size exclusion chromatography and dynamic light scattering and Lilian Hsiao for her assistance with multichannel confocal imaging. This work was supported by the NSF CDI Program (grant PHYS-0941227), the NIGMS (grant GM-069438), and a University of Michigan Rackham Merit Fellowship (to L.P.).

References

1. Shaw T, Winston M, Rupp CJ, Klapper I, Stoodley P. Commonality of elastic relaxation times in biofilms. Phys Rev Lett. 2004; 93:4.
2. Donlan RM, Costerton JW. Biofilms: Survival mechanisms of clinically relevant microorganisms. Clin Microbiol Rev. 2002; 15:167–193. [PubMed: 11932229]
3. Rasmussen B. Filamentous microfossils in a 3,235-million-year-old volcanogenic massive sulphide deposit. Nature. 2000; 405:676–679. [PubMed: 10864322]
4. Hall-Stoodley L, Costerton JW, Stoodley P. Bacterial biofilms: From the natural environment to infectious diseases. Nat Rev Microbiol. 2004; 2:95–108. [PubMed: 15040259]
5. Otto M. Staphylococcus epidermidis - the 'accidental' pathogen. Nat Rev Microbiol. 2009; 7:555–567. [PubMed: 19609257]
6. Rohde H, Frankenberger S, Zahringer U, Mack D. Structure, function and contribution of polysaccharide intercellular adhesin (PIA) to Staphylococcus epidermidis biofilm formation and pathogenesis of biomaterial-associated infections. Eur J Cell Biol. 2010; 89:103–111. [PubMed: 19913940]
7. Wilking JN. Biofilms as complex fluids. MRS Bull. 2011; 36:385–391.
8. Costerton JW, Stewart PS, Greenberg EP. Bacterial biofilms: A common cause of persistent infections. Science. 1999; 284:1318–1322. [PubMed: 10334980]
9. Hall-Stoodley L, Stoodley P. Evolving concepts in biofilm infections. Cell Microbiol. 2009; 11:1034–1043. [PubMed: 19374653]
10. Cheema MS, Rassing JE, Marriott C. The diffusion characteristics of antibiotics in mucus glycoprotein gels. J Pharm Pharmacol. 1986; 38:53P–53P.
11. Jefferson KK, Goldmann DA, Pier GB. Use of confocal microscopy to analyze the rate of vancomycin penetration through Staphylococcus aureus biofilms. Antimicrob Agents Chemother. 2005; 49:2467–2473. [PubMed: 15917548]
12. Chung HM, Cartwright MM, Bortz DM, Jackson TL, Younger JG. Dynamical system analysis of Staphylococcus epidermidis bloodstream infections. Shock. 2008; 30:518–526. [PubMed: 18317411]
13. O'Gara JP, Humphreys H. Staphylococcus epidermidis biofilms: importance and implications. J Med Microbiol. 2001; 50:582–587. [PubMed: 11444767]
14. Marrie TJ, Nelligan J, Costerton JW. A scanning and transmission electron microscopic study of an infected endocardial pacemaker lead. Circulation. 1982; 66:1339–1341. [PubMed: 7139907]
15. Nickel JC, Ruseska I, Wright JB, Costerton JW. Tobramycin resistance of Pseudomonas aeruginosa cells growing as a biofilm on urinary catheter material. Antimicrob Agents Chemother. 1985; 27:619–624. [PubMed: 3923925]
16. Brown MRW, Allison DG, Gilbert P. Resistance of bacterial biofilms to antibiotics a growth-rate related effect? J Antimicrob Chemother. 1988; 22:777–780. [PubMed: 3072331]
17. Mah T-FC, O'Toole GA. Mechanisms of biofilm resistance to antimicrobial agents. Trends Microbiol. 2001; 9:34–39. [PubMed: 11166241]
18. Fux CA, Costerton JW, Stewart PS, Stoodley P. Survival strategies of infectious biofilms. Trends Microbiol. 2005; 13:34–40. [PubMed: 15639630]
19. Costerton JW, Lewandowski Z, Caldwell DE, Korber DR, Lappin-Scott HM. Microbial biofilms. Annu Rev Microbiol. 1995; 49:711–745. [PubMed: 8561477]
20. Wolcott R, Dowd S. The role of biofilms: Are we hitting the right target? Plast Reconstr Surg. 2011; 127:28S–35S. [PubMed: 21200270]

21. Waters MS, Kundu S, Lin NJ, Lin-Gibson S. Microstructure and Mechanical Properties of In Situ Streptococcus mutans Biofilms. ACS Appl Mater Interfaces. 2013; 6:327–332. [PubMed: 24351115]
22. Rogers SS, van der Walle C, Waigh TA. Microrheology of Bacterial Biofilms In Vitro: Staphylococcus aureus and Pseudomonas aeruginosa. Langmuir. 2008; 24:13549–13555. [PubMed: 18980352]
23. Di Stefano A, D'Aurizio E, Trubiani O, Grande R, Di Campli E, Di Giulio M, Di Bartolomeo S, Sozio P, Iannitelli A, Nostro A, Cellini L. Viscoelastic properties of Staphylococcus aureus and Staphylococcus epidermidis mono-microbial biofilms. Microb Biotechnol. 2009; 2:634–641. [PubMed: 21255298]
24. Aggarwal S, Poppele EH, Hozalski RM. Development and testing of a novel microcantilever technique for measuring the cohesive strength of intact biofilms. Biotechnol Bioeng. 2010; 105:924–934. [PubMed: 19953669]
25. Aggarwal S, Hozalski RM. Effect of strain rate on the mechanical properties of Staphylococcus epidermidis biofilms. Langmuir. 2012; 28:2812–2816. [PubMed: 22217007]
26. Jones WL, Sutton MP, McKittrick L, Stewart PS. Chemical and antimicrobial treatments change the viscoelastic properties of bacterial biofilms. Biofouling. 2011; 27:207–215. [PubMed: 21279860]
27. Hohne DN, Younger JG, Solomon MJ. Flexible microfluidic device for mechanical property characterization of soft viscoelastic solids such as bacterial biofilms. Langmuir. 2009; 25:7743–7751. [PubMed: 19219968]
28. Vinogradov AM, Winston M, Rupp CJ, Stoodley P. Rheology of biofilms formed from the dental plaque pathogen Streptococcus mutans. Biofilms. 2004; 1:49–56.
29. Klapper I, Rupp CJ, Cargo R, Purvedorj B, Stoodley P. Viscoelastic fluid description of bacterial biofilm material properties. Biotechnol Bioeng. 2002; 80:289–296. [PubMed: 12226861]
30. Rupp CJ, Fux CA, Stoodley P. Viscoelasticity of Staphylococcus aureus biofilms in response to fluid shear allows resistance to detachment and facilitates rolling migration. Appl Environ Microbiol. 2005; 71:2175–2178. [PubMed: 15812054]
31. Pavlovsky L, Younger JG, Solomon MJ. In situ rheology of Staphylococcus epidermidis bacterial biofilms. Soft Matter. 2013; 9:122–131. [PubMed: 25544855]
32. Ganesan M, Stewart EJ, Szafranski J, Satorius AE, Younger JG, Solomon MJ. Molar mass, entanglement, and associations of the biofilm polysaccharide of Staphylococcus epidermidis. Biomacromolecules. 2013; 14:1474–1481. [PubMed: 23540609]
33. Stewart EJ, Satorius AE, Younger JG, Solomon MJ. Role of environmental and antibiotic stress on Staphylococcus epidermidis biofilm microstructure. Langmuir. 2013; 29:7017–7024. [PubMed: 23688391]
34. Rao W, Deng Z-S, Liu J. A review of hyperthermia combined with radiotherapy/chemotherapy on malignant tumors. Crit Rev Biomed Eng. 2010; 38:101–116. [PubMed: 21175406]
35. Issels RD, Lindner LH, Verweij J, Wust P, Reichardt P, Schem B-C, Abdel-Rahman S, Daugaard S, Salat C, Wendtner C-M, Vujaskovic Z, Wessalowski Rd, Jauch K-W, Durr HR, Ploner F, Baur-Melnyk A, Mansmann U, Hiddemann W, Blay J-Y, Hohenberger P. Neo-adjuvant chemotherapy alone or with regional hyperthermia for localised high-risk soft-tissue sarcoma: a randomised phase 3 multicentre study. Lancet Oncol. 2010; 11:561–570. [PubMed: 20434400]
36. Stewart PS, Rani SA, Gjersing E, Codd SL, Zheng Z, Pitts B. Observations of cell cluster hollowing in Staphylococcus epidermidis biofilms. Lett Appl Microbiol. 2007; 44:454–457. [PubMed: 17397487]
37. O'Neill KL, Fairbairn DW, Smith MJ, Poe BS. Critical parameters influencing hyperthermia-induced apoptosis in human lymphoid cell lines. Apoptosis. 1998; 3:369–375. [PubMed: 14646484]
38. Zerhouni EA, Parish DM, Rogers WJ, Yang A, Shapiro EP. Human heart: tagging with MR imaging-a method for noninvasive assessment of myocardial motion. Radiology. 1988; 169:59–63. [PubMed: 3420283]
39. Yang M-C, Scriven LE, Macosko CW. Some rheological measurements on magnetic iron oxide suspensions in silicone oil. J Rheol. 1986; 30:1015–1029.

40. Dzul SP, Thornton MM, Hohne DN, Stewart EJ, Shah AA, Bortz DM, Solomon MJ, Younger JG. Contribution of the Klebsiella pneumoniae capsule to bacterial aggregate and biofilm microstructures. Appl Environ Microbiol. 2011; 77:1777–1782. [PubMed: 21239544]
41. Crocker JC, Grier DG. Methods of digital video microscopy for colloidal studies. J Colloid Interface Sci. 1996; 179:298–310.
42. Marrie TJ, Costerton JW. Scanning and transmission electron microscopy of in situ bacterial colonization of intravenous and intraarterial catheters. J Clin Microbiol. 1984; 19:687–693. [PubMed: 6429190]
43. Berry GC. Thermodynamic and conformational properties of polystyrene. I. Light-scattering studies on dilute solutions of linear polystyrenes. J Chem Phys. 1966; 44:4550–4564.
44. Ioan CE, Aberle T, Burchard W. Solution properties of glycogen. 1. Dilute solutions. Macromolecules. 1999; 32:7444–7453.
45. Smith RL, Gilkerson E. Quantitation of glycosaminoglycan hexosamine using 3-methyl-2-benzothiazolone hydrazone hydrochloride. Anal Biochem. 1979; 98:478–480. [PubMed: 496014]
46. Smith PK, Krohn RI, Hermanson GT, Mallia AK, Gartner FH, Provenzano MD, Fujimoto EK, Goeke NM, Olson BJ, Klenk DC. Measurement of protein using bicinchoninic acid. Anal Biochem. 1985; 150:76–85. [PubMed: 3843705]
47. Desjardins, RP., Conklin, DS. Current Protocols in Molecular Biology. John Wiley & Sons; 2011. Microvolume Quantitation of Nucleic Acids.
48. Desjardins P, Conklin D. NanoDrop microvolume quantitation of nucleic acids. J Visualized Exp. 2010:e2565.
49. Provencher SW. A constrained regularization method for inverting data represented by linear algebraic or integral equations. Comput Phys Commun. 1982; 27:213–227.
50. Lu Q, Solomon MJ. Probe size effects on the microrheology of associating polymer solutions. Phys Rev E. 2002; 66:061504.
51. Shetty AM, Solomon MJ. Aggregation in dilute solutions of high molar mass poly(ethylene) oxide and its effect on polymer turbulent drag reduction. Polymer. 2009; 50:261–270.
52. Touhami A, Jericho MH, Beveridge TJ. Atomic force microscopy of cell growth and division in Staphylococcus aureus. J Bacteriol. 2004; 186:3286–3295. [PubMed: 15150213]
53. Sapan CV, Lundblad RL, Price NC. Colorimetric protein assay techniques. Biotechnol Appl Biochem. 1999; 29:99–108. [PubMed: 10075906]
54. Christensen GD, Simpson WA, Bisno AL, Beachey EH. Adherence of slime-producing strains of Staphylococcus epidermidis to smooth surfaces. Infect Immunol. 1982; 37:318–326. [PubMed: 6179880]
55. Davies D. Understanding biofilm resistance to antibacterial agents. Nat Rev Drug Discovery. 2003; 2:114–122. [PubMed: 12563302]
56. Kumar CG, Anand SK. Significance of microbial biofilms in food industry: a review. Int J Food Microbiol. 1998; 42:9–27. [PubMed: 9706794]
57. Qian Z, Sagers R, Pitt W. The effect of ultrasonic frequency upon enhanced killing of P. aeruginosa biofilms. Ann Biomed Eng. 1997; 25:69–76. [PubMed: 9124740]
58. Okuno K, Tuchiya K, Ano T, Shoda M. Effect of super high magnetic field on the growth of escherichia coli under various medium compositions and temperatures. J Ferment Bioeng. 1993; 75:103–106.
59. Pothakamury UR, Vega H, Zhang Q, Barbosa-Canovas GV, Swanson BG. Effect of growth stage and processing temperature on the inactivation of E. coli by pulsed electric fields. J Food Prot. 1996; 59:1167–1171.

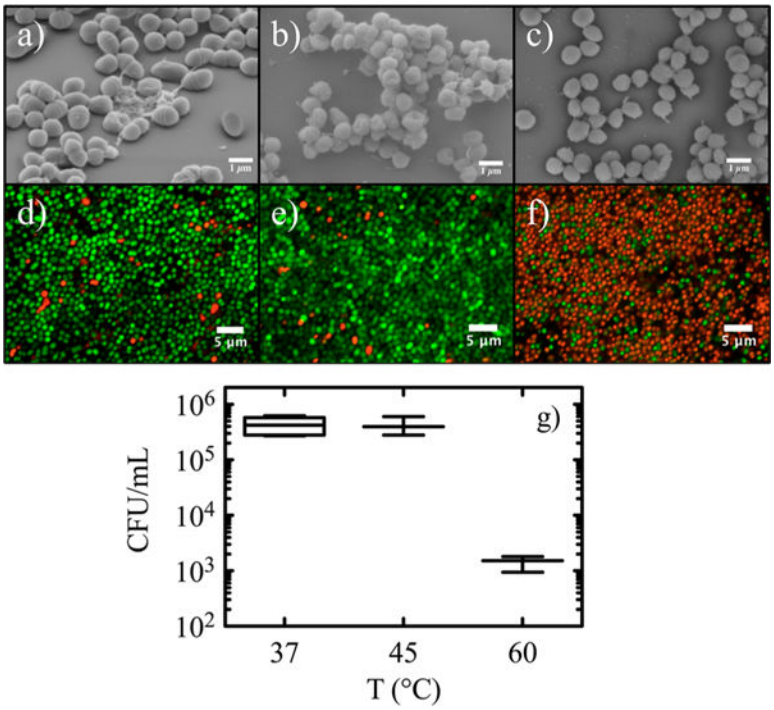

Figure 1.

Morphology and viability of *Staphylococcus epidermidis* bacterial cells after temperature treatment. Scanning electron microscopy micrographs show the external contours of individual cells after treatment at (a) 37, (b) 45, and (c) 60 °C. Confocal laser scanning microscopy shows the ratio of live (green) to dead (red) cells after treatment at (d) 37, (e) 45, and (f) 60 °C. (g) Quantitative growth cultures show the density of colony-forming units present per mL of media following the three different temperature treatments. Each sample was tested in triplicate, and error bars represent the standard error of the mean.

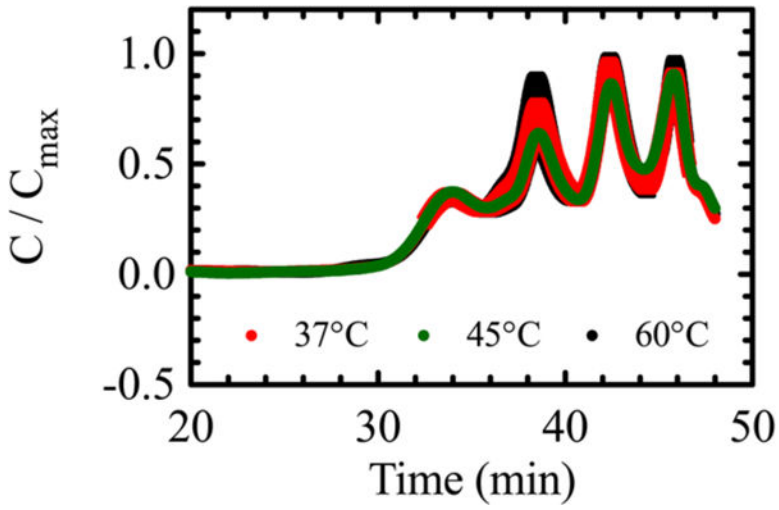

Figure 2.

Size exclusion chromatography of EPS as a function of temperature. Concentration detector curves for the SEC samples. Each temperature treatment was tested in triplicate, while the 37 °C control case consisted of six replicates. The results were normalized for each sample. Error bars represent the standard error of the mean.

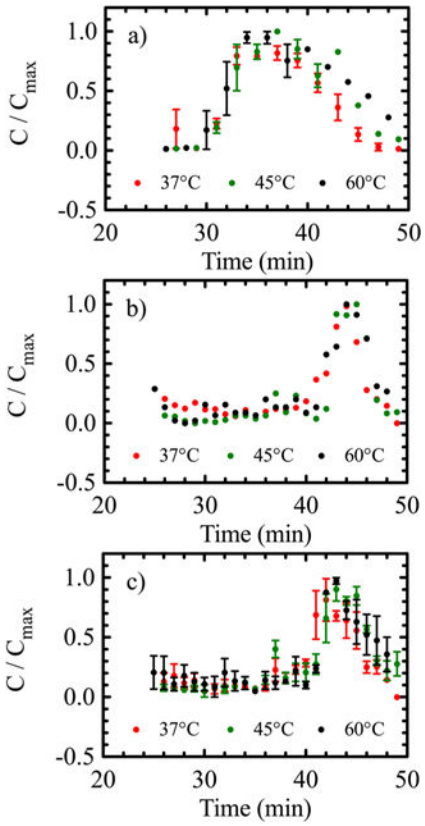

Figure 3.

Chemical composition of EPS as a function of temperature. The presence of (a) *N*-acetyl-glucosamine, (b) nucleic acid, and (c) protein in the SEC effluent fractions is shown as a function of temperature, as determined by various chemical assays. *N*-Acetyl-glucosamine assays were conducted in triplicate, while the remaining assays were single experiments. The protein is shown as an average concentration of two different assay techniques. The points were normalized for each sample. Error bars represent the standard error of the mean.

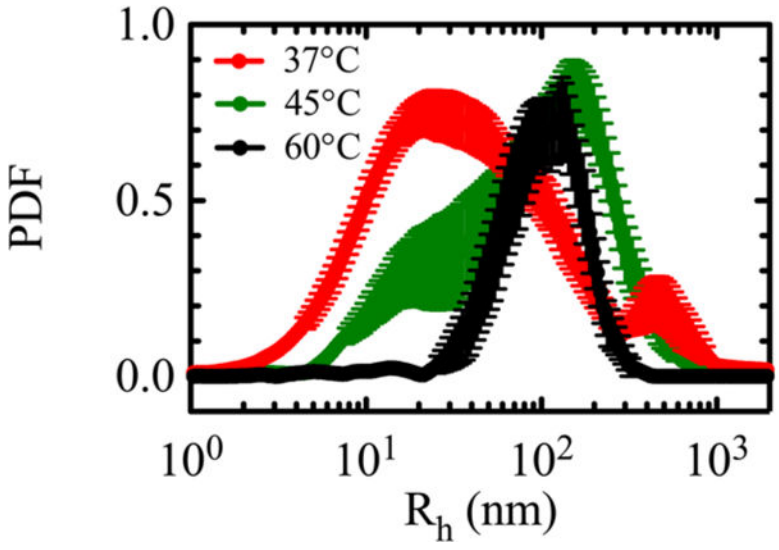

Figure 4.

Probability distribution of the hydrodynamic radius of the polymers in EPS as a function of temperature, determined via dynamic light scattering. Each temperature treatment was tested in triplicate, while the 37 °C control case consisted of six replicates. Results were normalized for each sample. Error bars represent the standard error of the mean.

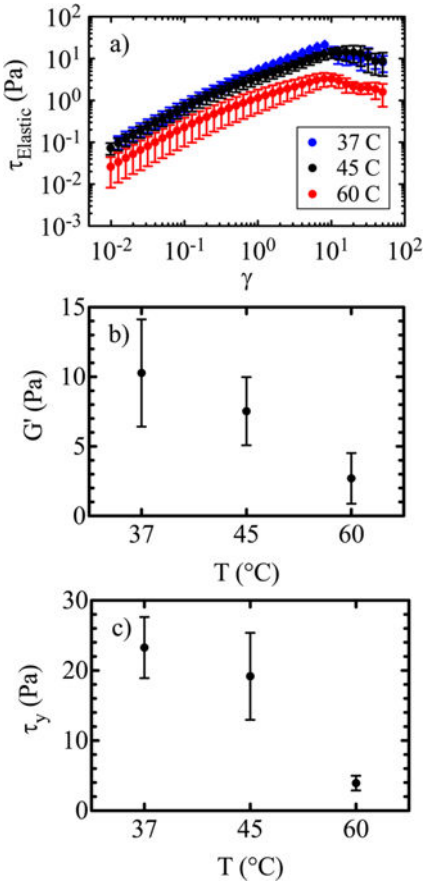

Figure 5.

Rheological characterization of *Staphylococcus epidermidis* biofilms as a function of temperature through parallel plate rheometry. (a) The shear stress ($\tau_{Elastic} = G' \times$ strain) as a function of the strain over the three temperatures of interest. The maximum point of each curve was taken as the yield stress. (b) The small strain elastic modulus of the biofilms at 37, 45, and 60 °C. (c) The yield stress (τ_y) of the biofilms at 37, 45, and 60 °C. Each measurement was made in triplicate, and error bars represent the standard error of the mean.

Table 1

Reproductive Health and Viability of Bacterial Cells Found via SEM and CLSM[a]

temp (°C)	% single cells (SEM)	% dividing pairs (SEM)	% dead cells (CLSM)
37	42.7 ± 2.3	57.3 ± 2.3	11.0 ± 3.5
45	97.2 ± 0.3	2.8 ± 0.3	10.4 ± 1.1
60	100 ± 0.0	0.0 ± 0.0	73.0 ± 3.4

[a]The percentage of single cells and percentage of dividing pairs are from three SEM images per temperature treatment and represent the cells with and without a dividing plane, respectively. The percentage of dead cells from the total cells present was determined using CLSM from three 3D volumes of biofilm per sample condition. Each result is displayed with the standard error of the mean.